JOURNAL OF GEOPHYSICAL RESEARCH, VOL. 115, D14117, doi:10.1029/2009JD012284, 2010

Temporal and spatial characteristics of fog occurrence over the Korean Peninsula

Yong Hee Lee,[1] Jeong-Soon Lee,[1] Seon Ki Park,[2] Dong-Eon Chang,[1] and Hee-Sang Lee[1]

Received 20 April 2009; revised 5 January 2010; accepted 10 March 2010; published 29 July 2010.

[1] In this study, fogs are classified based on the spatial and temporal characteristics over South Korea using the visibility data and the empirical orthogonal function (EOF) and wavelet analyses. With fog defined in terms of visibility (<1 km), the EOF analysis is performed to extract spatial distribution characteristics via dimension reduction, whereas the space-time wavelet expansion is applied to the EOF time series to specify the fog characteristics in the space of time versus scale (i.e., period in this study). The first EOF mode occupies 48.9% of total variance and shows the fog distribution covering almost entire areas of South Korea with one sign (+), except at the eastern coast and western part of the southern coast. The wavelet analysis reveals that this fog occurs based on meteorological conditions of various scales from daily to seasonal, thus classified as mixed fog. The second EOF mode, which occupies 19.5% of total variance, shows distinct separation of spatial distribution of fog, with a negative (−) sign in winter over northwestern coastal/inland, western coastal, and south central mountain areas of South Korea and a positive (+) sign in other seasons elsewhere. With cycles of 1–2 weeks and 1–2 months being dominant in the wavelet analysis, this fog is considered to be strongly affected by synoptic scale weather systems and monsoon. Fog over the positive area is mostly affected by monsoon and/or cyclonic frontal systems, thus classified as frontal fog, whereas that over the negative area is affected by the cold-core anticyclones moving over warm sea surface in winter or by radiative cooling, thus classified as steam fog (coastal/sea) or radiation fog (inland), respectively. The mountain area may have upslope fog because of orographic lifting. The third EOF mode, occupying 6.7% of total variance, depicts distinct spatial separation of fog distribution around the coastal areas with a negative (−) sign and in the inland areas with a positive (+) sign. The former, with a dominant 1–2 week cycle, is classified as sea fog affected by migratory anticyclones and monsoon in late spring and summer, while the latter, with a dominant diurnal variation, represents radiation fog under clear sky in autumn. It turns out that the combined EOF and wavelet analyses are useful to assess the detailed spatial and temporal characteristics of various types of fog occurrence in South Korea.

Citation: Lee, Y. H., J.-S. Lee, S. K. Park, D.-E. Chang, and H.-S. Lee (2010), Temporal and spatial characteristics of fog occurrence over the Korean Peninsula, *J. Geophys. Res.*, *115*, D14117, doi:10.1029/2009JD012284.

1. Introduction

[2] Fog, in a variety of formation types, sometimes brings about serious hazards to transportation using aircrafts, ships, and cars under poor visibility condition. Since major transportation facilities, such as airports, harbors, and trunk roads, are often constructed in fog-prone areas around the world, chances for accidents caused by reduced visibility always exist [e.g., *Whiffen*, 2001; *Whiffen et al.*, 2003]. South Korea recently had a tragic accident with a pileup of 29 cars and trucks on a major highway near the western coast because of dense fog with visibility of 50–60 m, leaving 11 dead and 50 injured.

[3] Previous studies on fog have focused on particular regions of frequent fog occurrence or on respective characteristics of radiation fog or advection fog (i.e., sea fog) [see *Meyer and Lala*, 1990; *Lewis et al.*, 2004]. This might be because fog is one of the meteorological phenomena greatly influenced by geographical characteristics and because the fog formation occurs from different causes.

[4] The Korean Peninsula, surrounded by seas on its three sides and featured by a complex topography, demonstrates strong regional characteristics in fog formation. Studies on fog formed over the Korean Peninsula have focused on

[1]Forecast Research Laboratory, National Institute of Meteorological Research, Korea Meteorological Administration, Seoul, Republic of South Korea.

[2]Center for Climate/Environment Change Prediction Research, Severe Storm Research Center, and Department of Environmental Science and Engineering, Ewha Womans University, Seoul, Republic of South Korea.

0148-0227/10/2009JD012284

indirect understanding of the fog formation by analyzing the relationship between the fog formation and other meteorological data, rather than direct understanding of the mechanism of fog formation [e.g., *Won et al.*, 2000; *Heo and Ha*, 2004]. *Kim and Lee* [1970] categorized fog regions in the Korean Peninsula based on different formation types and reported that the western and southern coastal areas are mostly affected by sea fog or frontal fog, the eastern coastal areas are affected by sea fog formed by a mixture of warm and cold ocean currents, and the inland areas are affected by radiation fog or frontal fog. The frontal fogs are related to cyclones or a monsoon front moving into the peninsula during spring and summer, while radiation fogs mostly occur in clear autumn days. *Kim and Yum* [2010] investigated the relationship between coastal/sea fogs at a western coastal area and synoptic pressure patterns over the Korean Peninsula. They found that coastal/sea fogs showed the highest occurrence under the North Pacific High (38%), followed by the Siberian High (28%) and migratory anticyclones (19%) and cyclones (14%).

[5] *Cho et al.* [2000] reported that the frequency of sea fog occurrence is at its maximum in July in all seas around the Korean Peninsula with the highest frequency over the Yellow Sea (YS), followed by the East China Sea (ECS) and the East Sea/Sea of Japan (ESJ). Among the three seas, the value of the surface air temperature (SAT) minus the sea surface temperature (SST) is the largest over the YS in July. According to *Kim and Yum* [2010], duration of sea fog extends more than 24 h regardless of season.

[6] *Zhang et al.* [2009] recently studied the mechanism of onset (April) and retreat (August) of sea fog over the YS. The onset is strongly linked to the land-sea differential heating that leads to formation of a shallow anticyclone over the cool YS and northern ECS, whereas the retreat is associated with large-scale changes in the East Asian monsoons. During the core fog season of the YS (May–July), persistent monsoonal southerlies blowing into the lower SST areas are the major source of sea fog over the YS.

[7] The monsoonal frontal systems cause fogs over the coastal and inland areas as well as the seas in Korea. The monsoon season brings heavy rainfall in Korea between middle or late June and July because of the stationary fronts (called Changma) formed between the North Pacific High and the Okhotsk High. When the Korean Peninsula is positioned in the northern part of the Changma front, cloud systems develop along the stationary front because of inflow of a cold and humid northeasterly from the Sea of Okhotsk, and thick fog often forms in the south and west coasts of the Korean Peninsula because of inflow of highly humid air. Highly dense fog most likely occurs on the stationary front after a light precipitation event, and the persistent fog event is often observed in the North Pacific High after a dry condition [*Heo and Ha*, 2004].

[8] Frontal fog forms in an inversion layer across the frontal surface when rainfall occurs in a warm air mass above and gets evaporated and supersaturated in a cold air mass below, under the condition of quite weak wind over a slowly moving cold front or a stationary front. Fog also forms easily when the cold air below the frontal surface has a lower temperature than the dew point of warm and moist air ascending the frontal surface [*Elliott*, 1988].

[9] Although some properties of fog are known in terms of formation mechanisms and associated synoptic environment, an accurate forecast of formation, duration, and intensity of fog is one of the most difficult problems that local forecasters are faced with [*Ballard et al.*, 1991]. This difficulty arises from the complexity on which the fog is dependent, including topography and microphysical and mesoscale processes in the boundary layer forced by related synoptic systems [*Croft et al.*, 1997].

[10] Studies on understanding the mechanism of fog and developing corresponding forecast skills have been performed using various resources including climate data, satellite data, and numerical models. Analyses using climate data have limitations in assessing dynamical features of fog formation and in revealing mesoscale temporal variability of the planetary boundary layer [*Croft et al.*, 1997], mainly because of coarse temporal and spatial resolutions. Satellite data have their own strength in that they cover coastal areas. However, they may not be available during night, and their capability to discern between lower clouds and fog is limited. Using Moderate Resolution Imaging Spectroradiometer data, *Bendix et al.* [2005] suggested a method to reduce errors in identifying the lower clouds and fog, but it is in an experimental stage.

[11] Numerical simulation studies had focused on radiation fog, which has a relatively clear formation process [e.g., *Taylor*, 1917; see a review by *Rao and O'Sullivan*, 2003]. *Bergot and Guedalia* [1994] performed a sensitivity test with a 1-D model to improve forecast of radiation fog. They noted that the forecast accuracy decreased when the atmospheric cooling is weak, in the case of fog occurrence in the middle or at the end of the night. For the advection-related sea fog and coastal fog, extensive studies have been performed on the relationship between the fog formation and synoptic field, because of the difficulties in observations and the nonlinear effect of advection term [*Leipper*, 1994; *Roach*, 1995; *Jhun et al.*, 1998; *Choi*, 2001].

[12] Even though the numerical modeling plays a key role in many forecast problems, the fog forecast still remains a laborious task. High-resolution observational data are essential for a reliable numerical forecast, but it is hard to obtain such data in the case of fog. In Korea, the visibility (i.e., the fog index) is observed with the naked eye in a manned observatory every 3 h. Although the aviation observatory provides instrumental visibility data collected every hour, practical use of such data is limited because of the insufficient amount of accumulation.

[13] Improving forecast accuracy of various types of fog, based on empirical and/or numerical approaches, is essentially dependent on a thorough understanding of the spatial and temporal characteristics of corresponding types of fog. In this study, the possibility of detailed assessment of such characteristics and classification of fogs that occurred over the Korean Peninsula (South Korea only) is investigated using the empirical orthogonal function (EOF) analysis [see *Lorenz*, 1956] and the wavelet analysis [see *Torrence and Compo*, 1998].

[14] A data set, consisting of a number of interrelated variables, can have its dimensionality reduced through the principal component analysis (i.e., the EOF analysis) while retaining existing variation as much as possible [see *Jolliffe*,

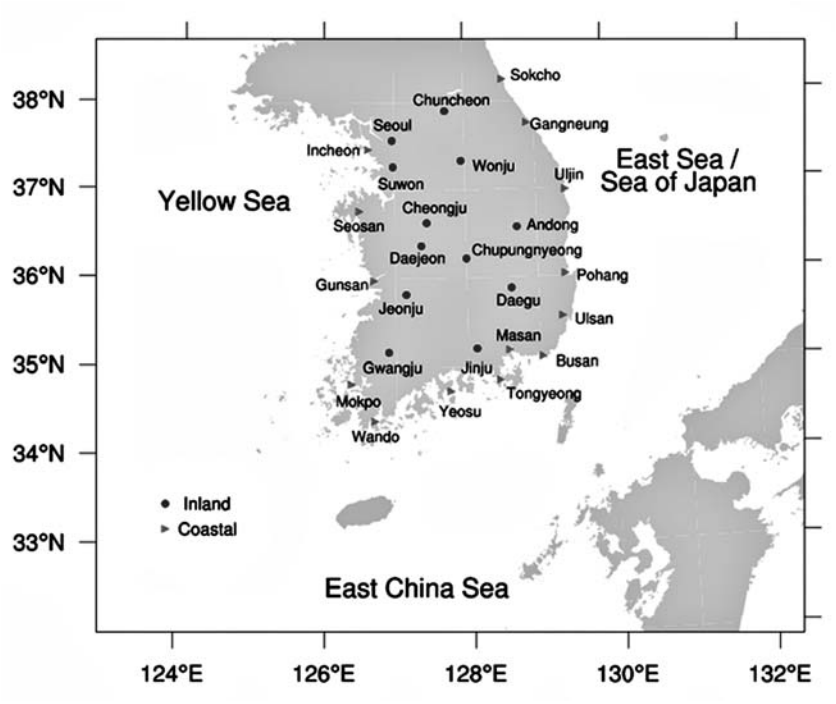

Figure 1. Station map for the visibility observation.

1990, 1993]. In other words, by transforming the original data to a new set of variables, one can extract a few independent variables (predictors or factors) that convey most of the variation in the original data.

[15] The EOF analysis has been applied to various studies in meteorology. *Fiorino and Correia* [2002] applied this method to filter mesoscale gravity wave signals from synoptic scale observations, while *Schmidli et al.* [2001] used it to reconstruct mesoscale precipitation fields from sparse observations. The wavelet transform has been increasingly used for separating different scales of variability. Recently, it has been implemented with respect to precipitation that has observational properties similar to fog, not consecutive in time unlike air temperature and wind direction [*Nolin and Hall-McKim*, 2006]. Wavelet transforms are also applied to convection over the tropical western Pacific to identify multiple timescales [*Weng and Lau*, 1994] and to precipitation over the United States to extract multiscale spatial and temporal variability [*Joseph et al.*, 2000]. However, either method has rarely been applied to fog analysis. This study is significant in that both the EOF and wavelet analyses are performed using fog data for the first time and that the occurrence of various fogs (e.g., frontal fog, radiation fog, and advection fog) is shown to be analyzed with a signal.

[16] In this study, aimed at providing background information to improve quantitative forecast of fog over South Korea, fogs are classified based on the spatial and temporal characteristics using the visibility data and the EOF and wavelet analyses. Noting that research on fogs and associated forecasts has been limited to case studies or monthly climate data analyses so far, it is expected through this study to extend the range of understanding on the fog occurrence characteristics to the viewpoint of various spatial and temporal scales.

2. Data and Methodology

[17] The visibility data were collected at a 3 h interval by the naked eye over the last 20 years (1987–2006). Here, fog is defined such that visibility is less than 1 km. Poor visibility cases (<1 km) caused by precipitation are excluded. Analyses are done for 26 observation stations (14 coastal and 12 inland) of the Korea Meteorological Administration (see Figure 1). The elevation of each station is shown in Table 1.

[18] The cloud data are used to investigate whether fog in autumn is essentially radiation fog. The cloud amount at the middle and lower layers is collected at the same sites of the

Table 1. Elevations of Observed Stations

Coastal (14)		Inland (12)	
Station	Elevation (m)	Station	Elevation (m)
Sokcho	0.0	Chuncheon	74.0
Gangneung	26.0	Seoul	85.5
Incheon	68.9	Wonju	149.0
Seosan	25.9	Suwon	36.0
Uljin	49.4	Cheongju	59.0
Pohang	5.0	Daejeon	68.3
Gunsan	26.0	Chupungnyeong	242.5
Ulsan	33.6	Andong	139.4
Masan	4.0	Daegu	57.6
Busan	69.2	Jeonju	51.0
Tongyeong	31.7	Gwangju	73.9
Mokpo	36.0	Jinju	21.3
Yeosu	67.0		
Wando	37.5		

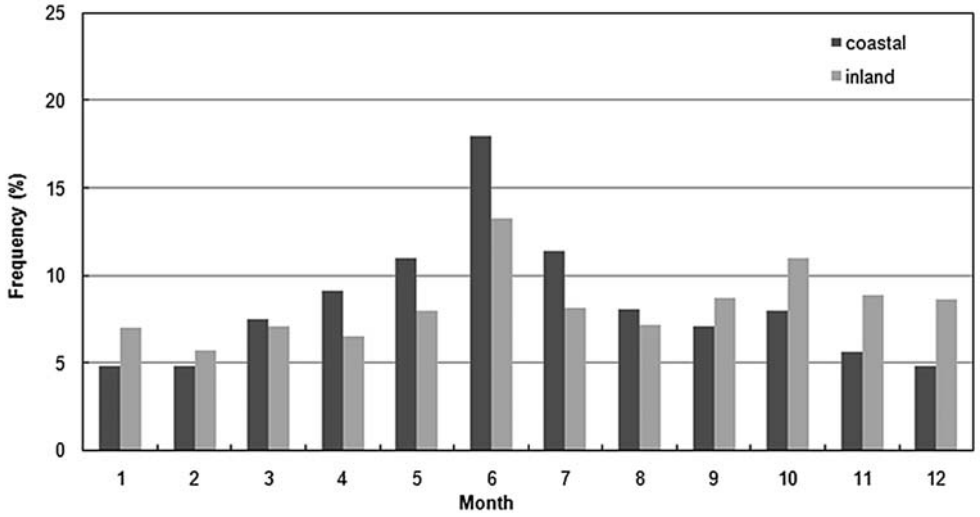

Figure 2. Distribution of monthly frequency (percentage) of fog occurrence showing that visibility is less than 1 km for the period 1987–2006.

visibility observation, with the same method (i.e., every 3 h by the naked eye), and is represented in a class from 0 (clear) to 10 (overcast). The clear day is defined as 2 or below, and the cloudy day is defined as 5 or above.

[19] To delineate the relevance to sea fog in the coastal area, the monthly SST and SAT distributions in the ESJ, YS, and ECS are used. The SSTs are based on the averaged monthly data of optimal interpolation SST (OISST) over the past 20 years (1987–2006) [see *Reynolds et al.*, 2002]. The resolution of OISST is 1° × 1°, and the grid points used for the SST are located at 125°–130°E, 32°–35°N in the ESJ; at 125°–127°E, 35°–38°N in the YS; and at 128°–130°E, 35°–38°N in the ECS. The SAT data are based on the averaged monthly data from the National Center for Environmental Prediction/National Center for Atmospheric Research (NCEP/NCAR) reanalysis for the past 20 years, at a resolution of 2.5° × 2.5° [*Kalnay et al.*, 1996]. The grid points for the SAT cover the same area as those for the SST. Note that some spatial errors are recognized because of the discrepancy in grid point locations between the SST data and the SAT data.

[20] With a purpose of investigating the spatial distribution characteristics of fogs, the EOF analysis is performed using the visibility data. It can be described simply by defining a set of time-spatial fog occurrence anomalies, $F(x, t)$, as

$$F(x,t) = \sum_{n=1}^{N} a_n(t) E_n(x), \tag{1}$$

where x represents the spatial component and $E_n(x)$ represents the eigenvector describing a particular spatial representation, i.e, nth EOF. The $a_n(t)$ is the amplitude (principal component (PC)) corresponding to E_n, and N is the number of stations. It is shown that the fog occurrence anomalies can be transformed to two variables: the EOF depicting spatial structures and the PC showing a time series of the corresponding EOF. Since the EOFs are orthogonal in space, there exists no space correlation between any two EOFs. Similarly, since the PCs are orthogonal in time, there is no simultaneous temporal correlation between any two PCs.

[21] In addition, the wavelet transform technique is applied to investigate the multiscale spatiotemporal characteristics of fog. The wavelet analysis transforms the time series data into the space of time versus scale (i.e., period in this study) to find major scales of fog occurrence variances and displays the variability of the concerned scale in terms of time. That is, the wavelet displays the components of a particular frequency at a particular time. A continuous wavelet transform is performed using the Morlet wavelet basis (ψ_0), which is represented as follows [*Morlet et al.*, 1982]:

$$\psi_0(\eta) = \pi^{-1/4} e^{i\omega_0\eta} e^{-\eta^2/2}, \tag{2}$$

where η is a nondimensional time parameter and ω_0 is a nondimensional oscillation frequency. Here, $\omega_0 = 6$ is used to satisfy the "admissibility condition" [*Farge*, 1992].

[22] The continuous wavelet transform, W_n, of the discontinuous observational data χ_n is defined as follows:

$$W_n(s) = \sum_{n'=0}^{N-1} \chi_{n'} \psi^* \left[\frac{(n' - n)\delta}{s} \right], \tag{3}$$

where *refers to a complex conjugate. By varying the wavelet scale, s, and translating along the localized time index, n, we can show the spatial characteristics and the temporal variations of the amplitude simultaneously [*Torrence and Compo*, 1998]. This study used the time series data obtained from respective modes in the EOF analysis (i.e., score).

[23] In applying the EOF and wavelet analyses, we used the visibility data collected in a 3 h interval every day. That is, each day includes data at 03, 06, 09, 12, 15, 18, and 21 local standard time (LST), resulting in 365 × 8 per year

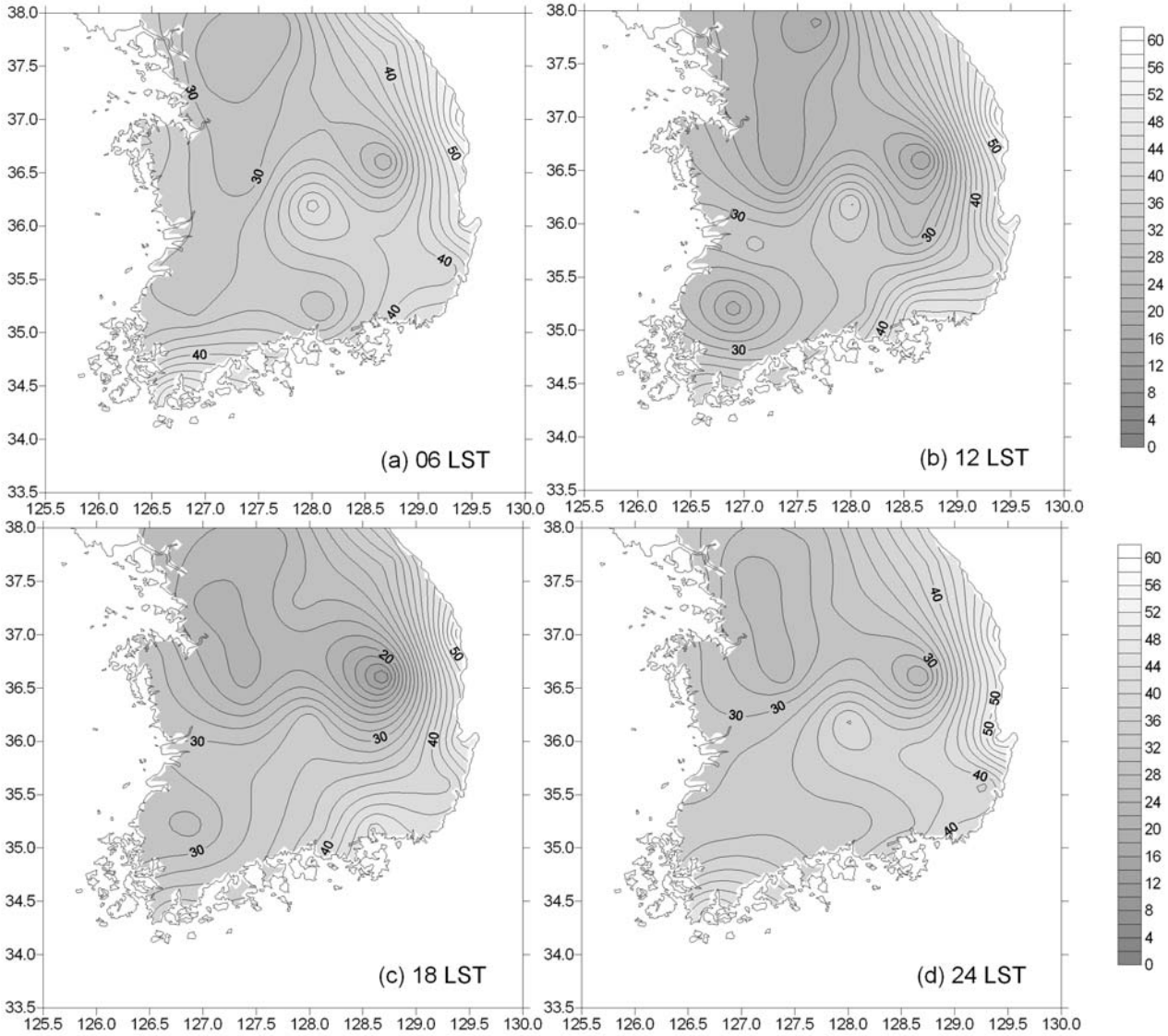

Figure 3. Frequency distribution of fog occurrence (percentage) at (a) 06, (b) 12, (c) 18, and (d) 24 LST for summer.

(excluding 29 February in a leap year). The data are accumulated every year on each Julian day for 20 years; hence, some specific time slot may have a maximum of 20 counts.

[24] In summary, this study is performed through the following steps: (1) to prepare a high-resolution (3 hourly) data set for fog occurrence in South Korea during last 20 years, (2) to perform the EOF analysis to the data set to extract major spatial distribution modes, (3) to apply the wavelet analysis to the EOF time series of each mode to assess multiscale spatiotemporal characteristics of fogs over South Korea, and (4) to analyze physical mechanisms related to such spatiotemporal characteristics of fogs.

3. Results

[25] As the Korean Peninsula is surrounded by seas on its three sides, we have supposed that frequency distributions are different from the coastal area to the inland and have analyzed the frequency distributions of respective forecast regions based on the 20 year data. Monthly fog frequency analysis in Figure 2 shows that June records the highest in fog occurrence in both coastal and inland areas. The fog occurrence is dominant in the coastal area during spring and summer (March–August) and in the inland area during autumn and winter (September–December). The inland shows relatively high fog occurrence in autumn, especially in October.

[26] The spatial distributions of fog occurrence at different local times (00, 06, 12, 18 LST) are shown for summer (Figure 3) and autumn (Figure 4). In Figure 3, the fog around the eastern coast and western part of the southern coast shows higher frequency than inland and varies rarely with time. It means that the fog occurrence in those coastal areas in summer is little affected by the diurnal variation (i.e., radiative heating and cooling). So the summer fog in the coastal area, excluding the western coast, is closely related to

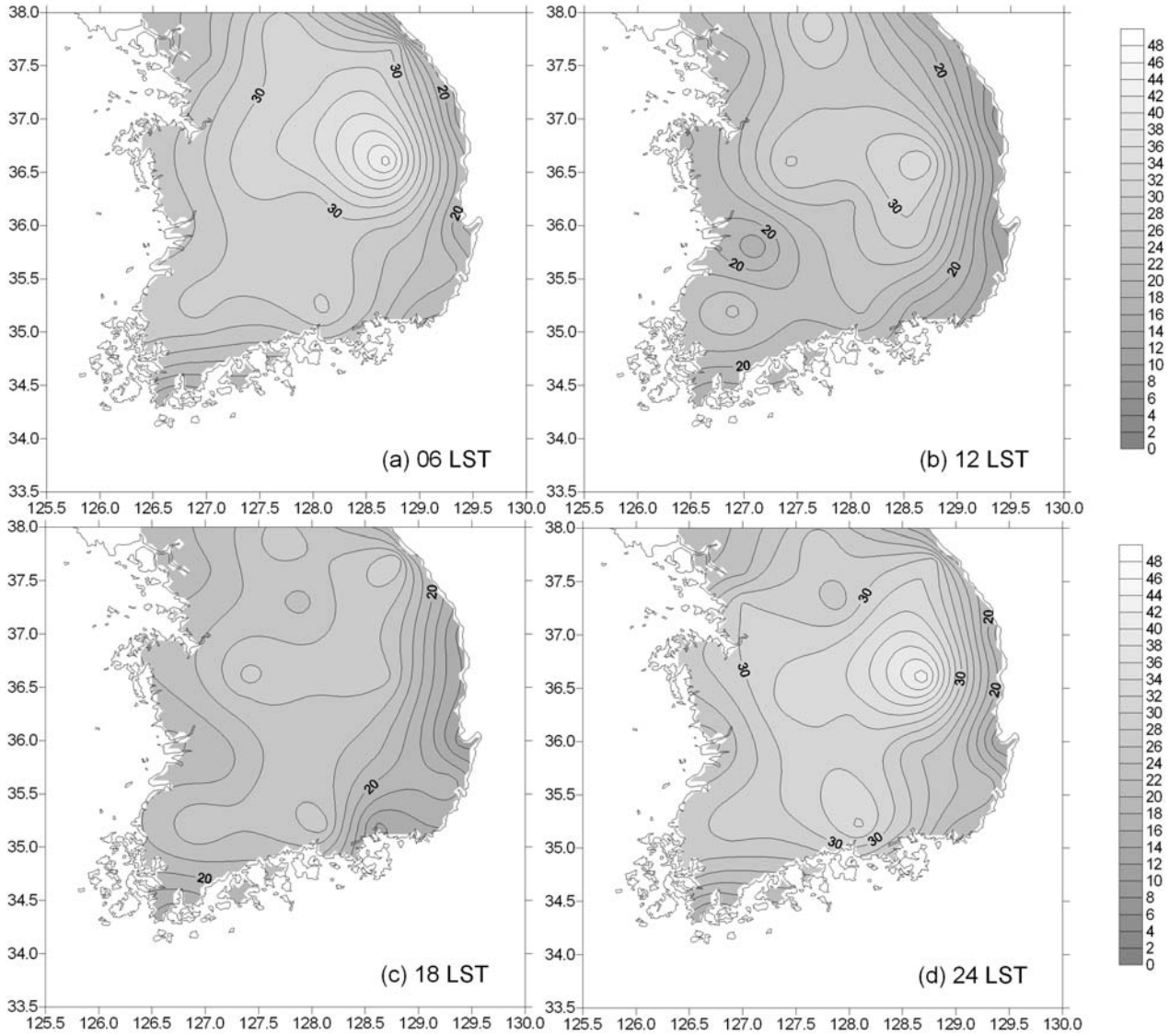

Figure 4. Same as Figure 3 except for autumn.

the advection fog that occurs when the moist air passes over a cool surface. Meanwhile, the autumn fog mostly occurs around the inland area (see Figure 4), especially Gyeongsangbukdo Province (mideastern parts of South Korea), and shows certain daily-range high frequency at 06 and 24 LST (nighttime) and low frequency at 12 and 18 LST (daytime). Hence, the nighttime inland fog in autumn may be related to the radiation fog, formed by the radiative cooling.

[27] It is noteworthy that the eastern and southern coastal areas show higher fog occurrence than the western coastal areas in summer (see Figure 3). This is contradictory to the result of *Cho et al.* [2000] that the west coast showed the highest occurrence of sea fog in Korea. Two possible reasons exist for this contradiction. First, their results show sea fog only, whereas our result may represent all types of fog including radiation fog, frontal fog, precipitation fog, advection fog (from nonsea source), lowered stratus, etc., as well as sea fog. Second, on the western coast, we have only 4 observation sites (all in the mainland), while they had 11 sites including eight stations over islands in the YS, focusing mainly on sea fog observations (compare Figure 1 herein and Figure 2 from the work of *Cho et al.* [2000]). The ESJ has almost no island where meteorological observation may be available, except Ullungdo.

[28] To investigate the relationship between the fog occurrence and temperature in the coastal area, monthly SST and SAT distributions over the three seas are examined. Sea fog forms when warm air traveling over a relatively cool sea surface gets cooled and supersaturated. When the SST is lower than the SAT, the potential for fog formation is great [*Cho et al.*, 2000]. Figure 5 shows monthly SST and SAT averaged for the last 20 years. The SST is lower than the SAT over the ESJ and the ECS from May to July and over the YS from April to July. It is noted that the YS, which has strong tidal mixing, shows the largest difference between the SST and SAT in summer.

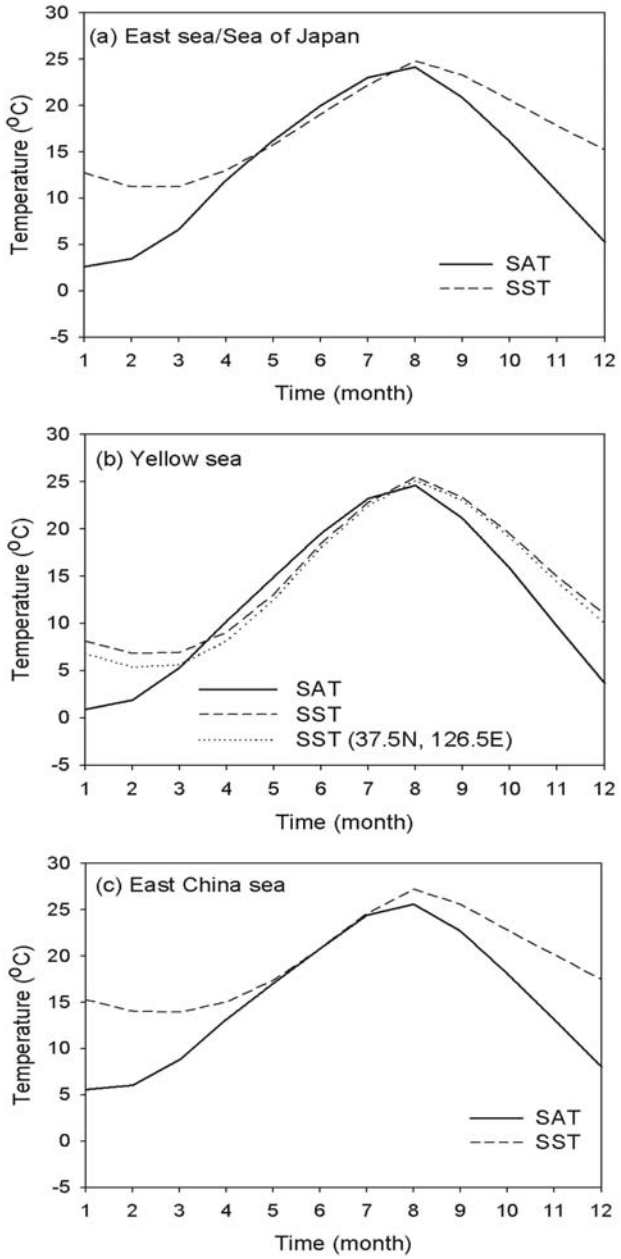

Figure 5. Sea surface temperature (SST; dashed line) and surface air temperature (SAT; solid line) in the (a) East Sea/Sea of Japan, (b) Yellow Sea, and (c) East China Sea.

[29] Our results in Figure 5 seem to be contradictory to those in Figure 3 in that the YS shows relatively lower fog occurrence in summer even with a much larger value in SAT-SST than the ECS and ESJ. As mentioned earlier, our results contain not only sea fog but also other types of fogs that may be observable in the coastal areas. This is supported by *Choi* [2001], who reported that, with the existence of a cool pool of seawater in the open sea, not only sea fog can form because of direct cooling and saturation of air over the sea surface but also coastal (radiation) fog can form in the coast because of nocturnal cooling of the ground surface and moist air advected from the sea.

[30] With general features of fog in Korea examined, more specific spatial and temporal characteristics of the fog occurrence are investigated though the EOF and wavelet analyses. Figures 6–8 illustrate results from the EOF analyses, such as the EOF (i.e., spatial structure) and the PC (i.e., time series of corresponding EOF; represented in 3 h interval) (a and b, respectively), and results from the wavelet analyses, including the local and global wavelet power spectrum (c and d, respectively) in the space of time versus period. In the local power spectrum (Figures 6c, 7c, and 8c), the thick contour encloses regions of the confidence level larger than 90%. In the global spectrum (Figures 6d, 7d, and 8d), the confidence level of 95% is shown as a dashed line. Although the analyses are done for Julian days, the x axes of Figures 6–8 are depicted in terms of month for simplicity.

[31] In Figure 6, the first loadings (eigenvector elements [*Wilks*, 1995]) of EOF analysis on the fog frequency are illustrated. The first EOF mode, which occupies 48.9% of total variances, is represented with one sign (+) across almost entire areas of South Korea, except at the eastern coast and western part of the southern coast where small (−) values near zero appear (Figure 6a). This implies that large-scale changes affect the peninsula-wide fog occurrence with locally different characteristics under meteorological conditions of various temporal scales (see discussion in Figure 6c). The time series of the first mode retain almost the same sign (+) throughout the year with maxima in June and relatively high amplitudes in autumn (September–November) (Figure 6b). The overall variations in the PC are similar to those in the monthly fog frequency analysis (compare Figure 2). In the local power spectrum, a diurnal variation is dominant throughout the year with relevant control by 2 week to 2 month cycles, mostly significant at the confidence level of 90% (Figure 6c). It suggests that this kind of fog can occur under meteorological conditions of various scales (from daily to seasonal); thus, it can be classified as mixed fog. However, at the east coast and western part of the southern coast, small values in spatial pattern (see Figure 6a) should result in small values in power spectrum (see Figure 6c). Therefore, at those coastal areas, the fog occurrence has little diurnal variation, which is consistent with diurnal variation of fog occurrence in those areas in summer, as shown in Figure 3. The global spectrum shows the 1 day cycle and other cycles (longer than 1 week) are significant at the confidence level of 95%, thus confirming that the fog over entire areas of South Korea occurs from various scales (Figure 6d). In summary, the majority of fogs (>48%) that are observed over almost entire areas of South Korea except at the aforementioned coastal areas, throughout the year, are essentially mixed fog formed by meteorological conditions of various scales, e.g., daily scale (radiation fog), 1–2 week scale (large-scale synoptic systems), and 1–2 month scale (monsoon front, subtropical high, etc.), which can occur simultaneously at different areas in different types.

[32] Figure 7 depicts the second mode of EOF that occupies 19.5% of total variance. It illustrates distinct separation of spatial fog distribution, with a negative (−) sign over Gyeonggido Province (northwestern coastal/inland areas of South Korea), the west central coast, and south central inland (Mt. Jiri) and a positive (+) sign elsewhere (see Figure 7a). The time series of the second mode shows

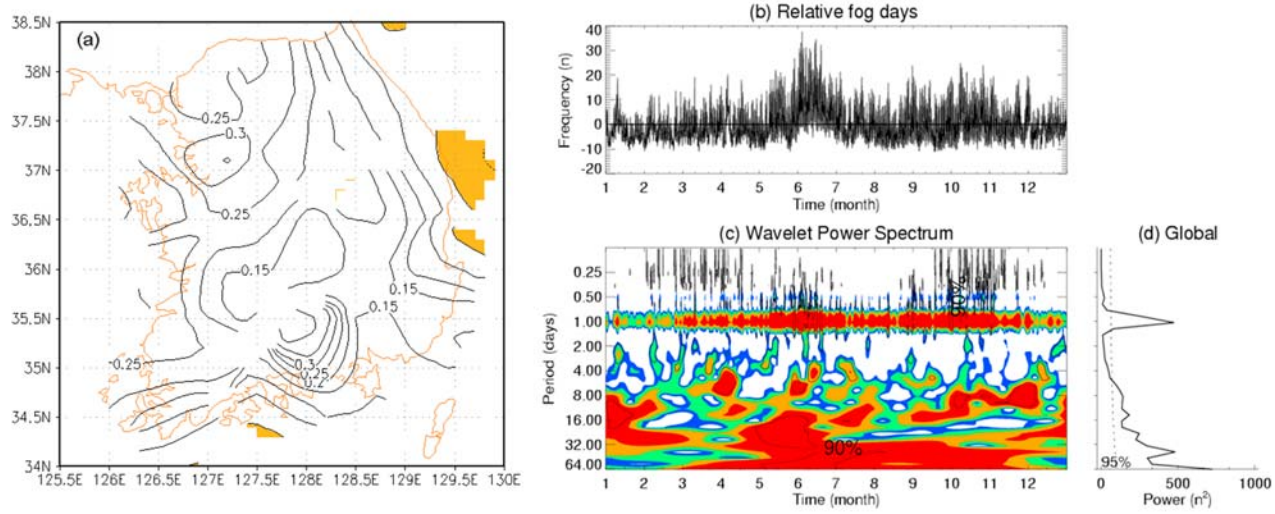

Figure 6. (a) Spatial distribution of the first mode. (b) Time series of the first scores of the relative fog frequency in the EOF analysis. (c) Local and (d) global wavelet power spectrum of Figure 6b using the Morlet wavelet.

negative (−) values during winter and positive (+) values in the other seasons with maximum amplitude in summer (Figure 7b). Cycles of 1–2 weeks and 1–2 months are dominant from late spring to early summer in the local power spectrum (Figure 7c). The global spectrum also supports this result at the confidence level of 95% (Figure 7d). Therefore, this fog is considered to be strongly affected by synoptic-scale weather systems (1–2 week cycle) and the monsoon system (1–2 month cycle). Note that the monsoon front is one of the major systems that affect the Korean Peninsula in early summer. Fog over the positive area is mostly affected by monsoon and/or cyclonic frontal systems, thus classified as frontal fog, whereas that over the negative area is mostly affected by the cold-core anticyclones moving over warm sea surface in winter or by radiative cooling, thus classified as steam fog (coastal/sea) or radiation fog (inland). However, the Jiri Mountain area shows the possibility of upslope fog caused by orographic lifting.

[33] *Heo and Ha* [2004] reported that fogs at southern and eastern coasts of South Korea mainly occur when frontal systems or a stationary (Changma) front move in. Our wavelet analysis captures features of frontal systems in late spring and early summer with a 1–2 week cycle and the Changma front from late June to July with a 1–2 month cycle. *Kim and Yum* [2010] showed that, in a western coast area, coastal fogs (i.e., radiation fog, frontal fog, etc.) were frequent in winter and warm water (steam) fog was frequent from January to May. This also supports our results that a

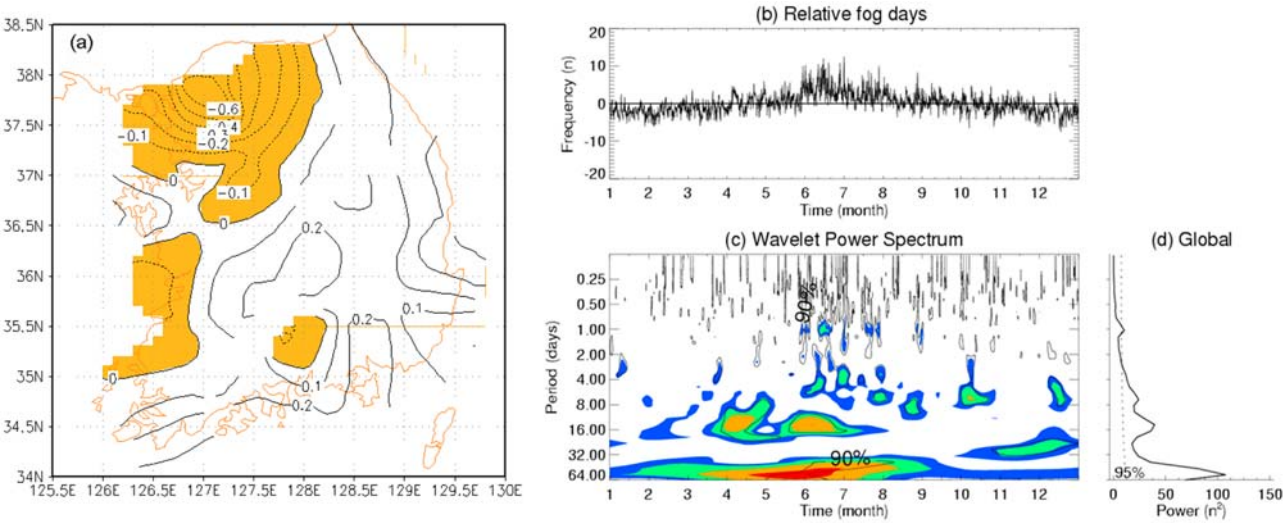

Figure 7. Same as Figure 6 except for the second mode.

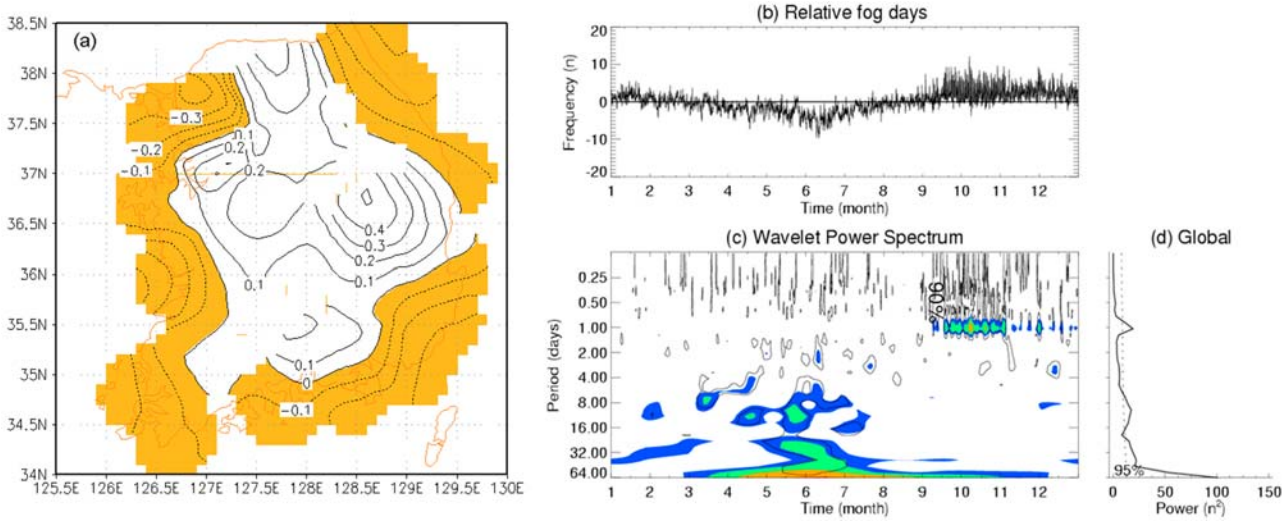

Figure 8. Same as Figure 6 except for the third mode.

good portion of negative loadings in winter are related to steam fog, while coastal fogs also are included.

[34] Properties of the third EOF mode, occupying 6.7% of total variance, are shown in Figure 8. It depicts clear spatial separation of fog distribution around the coastal areas with a negative (−) sign and in the inland areas with a positive (+) sign (Figure 8a). The former shows a high amplitude from late spring to summer, and the latter shows in autumn (Figure 8b). In the local wavelet spectrum, cycles of 1–2 weeks and 1–2 months are dominant from late spring to midsummer (late April–July), while a diurnal variation is clearly displayed in autumn (Figure 8c). This feature is also supported from the global spectrum (Figure 8d). The negative loadings in the coastal areas are classified as sea fog affected by migratory anticyclones and monsoon [see *Cho et al.*, 2000], whereas the positive loadings in the inland present radiation fog under clear sky.

[35] It is reported that the occurrence of coastal fogs of the Korean Peninsula from late spring to summer is strongly affected by migratory anticyclones that move in a period of 1–2 weeks [*Heo and Ha*, 2004]. This feature is well presented in our wavelet analyses (Figures 8c and 8d). Migratory anticyclones affecting the Korean Peninsula include one detached from the Siberian High and then moving from China, one separated from the North Pacific High, and one isolated from the Okhotsk High.

[36] Radiation fog occurs when the surface temperature falls down in a clear night, attributed to radiative cooling, the air around the surface becomes saturated, and the surplus vapor condenses [*Roach et al.*, 1976]. To clarify the relationship between the diurnal variation properties in autumn and radiation fog, the daily frequency distribution of fog occurrence under different sky conditions in terms of the middle and lower clouds over the past 20 years is investigated (Figure 9). The clear day is defined as 20% or less while the cloudy day is defined as 50% or more in cloud amount. The coastal area has a similar frequency distribution in both the clear and cloudy days during summer and winter, while having more clear days during spring and autumn (Figure 9a). The inland area has a similar frequency distribution in both the clear and cloudy days during summer, while having relatively more clear days during spring and autumn (Figure 9b). Furthermore, the inland area has relatively more clear days in autumn than in spring. Therefore, it can be considered that the autumn fog is closely related to radiation fog, supporting our results with the third EOF mode.

4. Conclusions

[37] Forecasting formation, duration, and intensity of fog is a challenging problem. For improving fog forecast, better understanding of spatial and temporal characteristics of fog occurrence is essential. However, such efforts have been limited to case studies on specific fog types at limited locations or studies based on analyses of monthly climate data. In this study, aimed at providing a framework to improve quantitative forecast of fog over South Korea, fogs are classified based on the spatial and temporal characteristics using the visibility data and the EOF and wavelet analyses.

[38] The visibility and cloud amount data were collected at a 3 h interval for 20 years at 26 observation stations (14 coastal and 12 inland). The monthly sea surface temperature and surface air temperature data over three seas around the Korean Peninsula are also used. The SSTs are based on the averaged monthly data of optimal interpolation SST over the past 20 years (1987–2006). The SAT data are based on the averaged monthly data of NCEP/NCAR reanalysis for the past 20 years.

[39] Fog is defined in terms of visibility (<1 km), and poor visibility caused by precipitation is excluded. General features of fog occurrence over South Korea include the following.

[40] 1. Fog occurrence is the highest in June in both coastal and inland areas and is dominant during spring and summer in the coastal area and during autumn and winter in the inland area.

[41] 2. The fog occurrence around the eastern coast and western part of the southern coast in summer shows higher frequency than inland and varies rarely with time (i.e., little affected by the diurnal variation). Therefore, it is closely

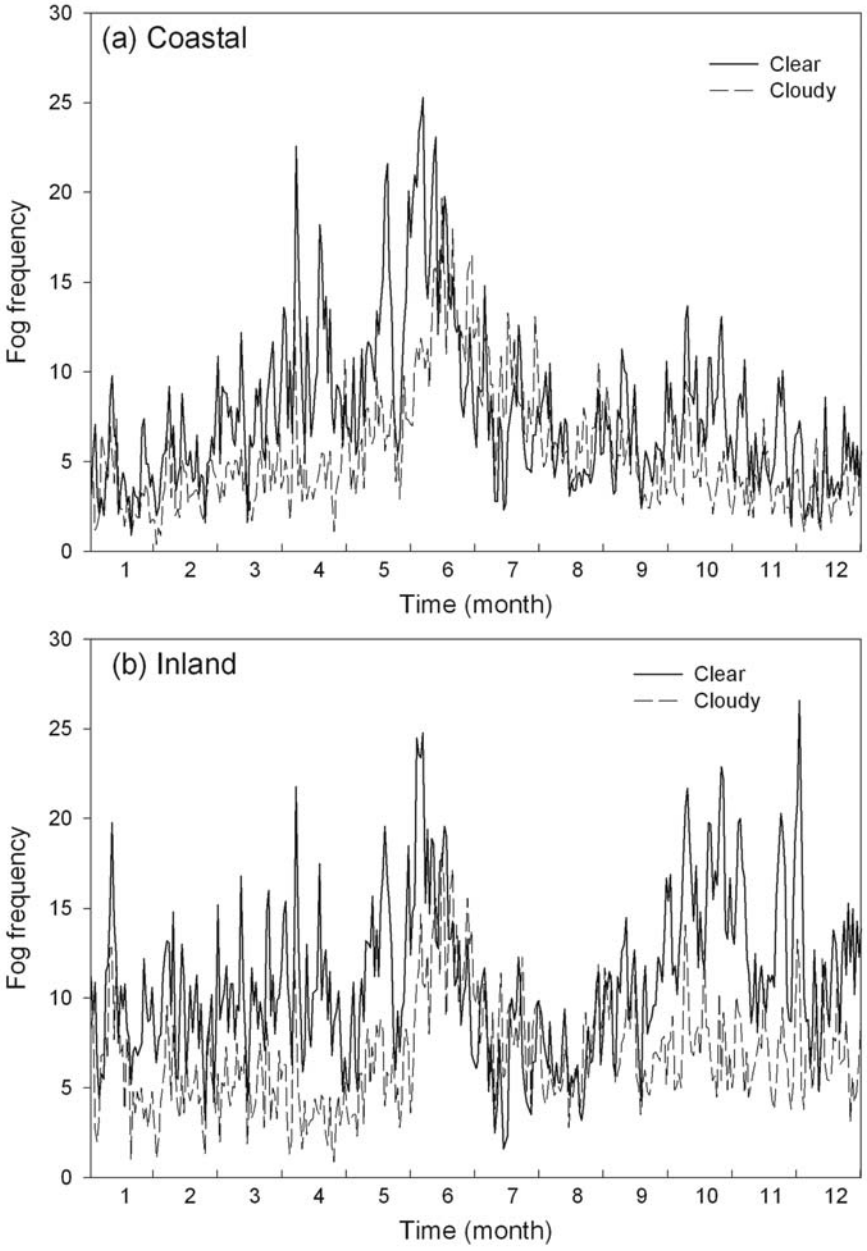

Figure 9. Fog frequency in terms of cloud amount (clear and cloudy) on the (a) coastal and (b) inland regions.

related to the sea (advection) fog. The autumn fog mostly occurs in the inland with high frequency at nighttime and low frequency at daytime. Hence, it is related to the radiation fog.

[42] 3. The Yellow Sea has the largest magnitude of SAT-SST in summer than the other seas, implying greater potential for sea fog occurrence. However, the frequency of coastal fog, which includes various fog types, is higher in the coastal areas of the East Sea/Sea of Japan and the East China Sea than those in the YS.

[43] The empirical orthogonal function analysis is performed to the visibility data to extract spatial distribution characteristics via dimension reduction, whereas the wavelet analysis is applied to the EOF time series to specify the multiscale spatiotemporal characteristics of fog occurrence in the space of time versus scale (i.e., period in this study) via space-time wavelet expansion. The spatiotemporal structures of fog over South Korea thus obtained are compared to previous studies and general features examined here and are used to classify fog occurrence based on spatial distributions, periods, and scales of meteorological forcing and to understand physical mechanisms of formation.

[44] The first EOF mode occupies 48.9% of total variance and shows the fog distribution covering almost entire areas of South Korea with one sign (+), except at the eastern coast and western part of the southern coast. The wavelet analysis reveals that this fog occurs based on meteorological conditions of various scales from daily to seasonal, thus classified

as mixed fog. Here, "mixed fog" occurs from meteorological conditions of various scales such that it may include radiation fog in a daily scale, frontal fog in weekly and monthly scales, warm/cold water fog in a weekly scale, etc. The majority of fog occurrence in South Korea is essentially affected by this mixed fog throughout the year, which can occur simultaneously at different areas in different types.

[45] The second EOF mode, which occupies 19.5% of total variance, shows distinct separation of spatial distribution of fog, with a negative (−) sign in winter over northwestern coastal/inland (Gyunggido Province), western coastal, and south central mountain (Mt. Jiri) areas of South Korea and a positive (+) sign in other seasons elsewhere. Cycles of 1–2 weeks and 1–2 months are dominant in the wavelet analysis, and this fog is considered to be strongly affected by synoptic scale weather systems and monsoon. Fog over the positive area is mostly affected by monsoon and/or cyclonic frontal systems, thus classified as frontal fog, while that over the negative area is affected by the cold-core anticyclones moving over warm sea surface in winter or by radiative cooling, thus classified as steam fog (coastal/sea) or radiation fog (inland), respectively. The mountain area may have upslope fog attributed to orographic lifting.

[46] The third EOF mode, occupying 6.7% of total variance, depicts distinct spatial separation of fog distribution around the coastal areas with a negative (−) sign and in the inland areas with a positive (+) sign. The former, with a dominant 1–2 week cycle, is classified as sea fog affected by migratory anticyclones and monsoon in late spring and summer, whereas the latter, with a dominant 1 day cycle, represents radiation fog under clear sky in autumn.

[47] It turns out that the combined EOF and wavelet analyses are useful to assess the detailed spatial and temporal characteristics of various types of fog occurrence in South Korea. On the basis of the results obtained in this work, further study is planned for detailed analysis on the relationship between the occurrence mechanisms and geographical and/or topographical characteristics.

[48] **Acknowledgments.** This study was mainly performed under the support of the National Institute of Meteorological Research of the Korea Meteorological Administration under a major project (NIMR-2009-B-1). S. K. Park was partly supported by the Advanced Basic Research Laboratory Program (R14-2002-031-01002-0) of the Korea Science and Engineering Foundation and by the Ministry of Education, Science, and Technology, Korea, through National Research Foundation grant 2009-0083527. Wavelet software was provided by C. Torrence and G. Compo and is available at http://atoc.colorado.edu/research/wavelets/.

References

Ballard, S. P., B. W. Golding, and R. N. B. Smith (1991), Mesoscale model experimental forecasts of the Harr of northeast Scotland, *Mon. Weather Rev.*, *119*, 2107–2123, doi:10.1175/1520-0493(1991)119<2107:MMEFOT>2.0.CO;2.

Bendix, J., B. Thies, J. Cermak, and T. Nauß (2005), Ground fog detection from space based on MODIS daytime data—A feasibility study, *Weather Forecast.*, *20*, 989–1005, doi:10.1175/WAF886.1.

Bergot, T., and D. Guedalia (1994), Numerical forecasting of radiation fog. Part I: Numerical model and sensitivity tests, *Mon. Weather Rev.*, *122*, 1218–1230, doi:10.1175/1520-0493(1994)122<1218:NFORFP>2.0.CO;2.

Cho, Y.-K., M.-O. Kim, and B.-C. Kim (2000), Sea fog around the Korean Peninsula, *J. Appl. Meteorol.*, *39*, 2473–2479, doi:10.1175/1520-0450(2000)039<2473:SFATKP>2.0.CO;2.

Choi, H. (2001), Numerical prediction on fog formation affected by the Yellow Sea and mountain, *J. Korean Meteorol. Soc.*, *36*, 261–282.

Croft, P. J., R. L. Pfost, J. M. Medilin, and G. A. Johnson (1997), Fog Forecasting for the Southern region: A conceptual model approach, *Weather Forecast.*, *12*, 545–556, doi:10.1175/1520-0434(1997)012<0545:FFFTSR>2.0.CO;2.

Elliott, G. (1988), *Weather Forecasting, Rules, Techniques and Procedures*, 153 pp., American, Boston, Mass.

Farge, M. (1992), Wavelet transforms and their applications to turbulence, *Annu. Rev. Fluid Mech.*, *24*, 395–458, doi:10.1146/annurev.fl.24.010192.002143.

Fiorino, S. T., and J. Correia Jr. (2002), Analysis of a mesoscale gravity wave event using empirical orthogonal functions, *Earth Interact.*, *6*, 1–19, doi:10.1175/1087-3562(2002)006<0001:AOAMGW>2.0.CO;2.

Heo, K. Y., and K. J. Ha (2004), Classification of synoptic pattern associated with coastal fog around the Korean Peninsula (in Korean), *J. Korean Meteorol. Soc.*, *19*, 541–556, doi:10.3346/jkms.2004.19.4.541.

Jhun, J. G., E. J. Lee, S. A. Ryu, and S. H. Yoo (1998), Characteristics of regional fog occurrence and its relation to concentration of air pollutants in South Korea (in Korean), *J. Korean Meteorol. Soc.*, *34*, 486–496.

Jolliffe, I. T. (1990), Principal component analysis: A beginner's guide-I. Introduction and application, *Weather*, *45*, 375–382.

Jolliffe, I. T. (1993), Principal component analysis: A beginner's guide-II. Pitfalls, myths and extensions, *Weather*, *48*, 246–253.

Joseph, R., M. Ting, and P. Kumar (2000), Multiple-scale spatio-temporal variability of precipitation over the coterminous United States, *J. Hydrometeorol.*, *1*, 373–392, doi:10.1175/1525-7541(2000)001<0373:MSSTVO>2.0.CO;2.

Kalnay, E., et al. (1996), The NCEP/NCAR 40-Year Reanalysis Project, *Bull. Am. Meteorol. Soc.*, *77*, 437–472, doi:10.1175/1520-0477(1996)077<0437:TNYRP>2.0.CO;2.

Kim, C. K., and S. S. Yum (2010), Local meteorological and synoptic characteristics of the fogs formed over Incheon International Airport in the west coast of Korea, *Adv. Atmos. Sci.*, *27*(4), 761–776, doi:10.1007/s00376-009-9090-7.

Kim, S. S., and N. Y. Lee (1970), On the classification of the fog regions of Korea, *J. Korean Meteorol. Soc.*, *6*, 15–29.

Leipper, D. F. (1994), Fog on the U.S. West Coast: A review, *Bull. Am. Meteorol. Soc.*, *75*, 229–348, doi:10.1175/1520-0477(1994)075<0229:FOTUWC>2.0.CO;2.

Lewis, J. M., D. Koracin, and K. T. Redmond (2004), Sea fog research in the United Kingdom and United States, *Bull. Am. Meteorol. Soc.*, *85*, 395–408, doi:10.1175/BAMS-85-3-395.

Lorenz, E. N. (1956), Empirical orthogonal functions and statistical weather prediction, Sci. Rep. 1, Statistical Forecasting Project, *Doc. 110268*, 49 pp., MIT Defense Doc. Cent., Cambridge, Mass.

Meyer, M. B., and G. G. Lala (1990), Climatological aspects of radiation fog occurrence at Albany, New York, *J. Clim.*, *3*, 577–586, doi:10.1175/1520-0442(1990)003<0577:CAORFO>2.0.CO;2.

Morlet, J., G. Arens, I. Forgeau, and D. Giard (1982), Wave propagation and sampling theory, *Geophysics*, *47*, 222–236, doi:10.1190/1.1441329.

Nolin, A. W., and E. Hall-McKim (2006), Characteristic frequencies of monsoon precipitation in Arizona and New Mexico, *Mon. Weather Rev.*, *134*, 3774–3781, doi:10.1175/MWR3244.1.

Rao, G. V., and J. O'Sullivan (2003), A review of some recent radiation fog prediction studies and the results of integrating a simple numerical model to predict radiation fog over Brunei, *Pure Appl. Geophys.*, *160*, 239–250, doi:10.1007/s00024-003-8775-6.

Reynolds, R. W., N. A. Rayner, T. M. Smith, D. C. Stokes, and W. Wang (2002), An improved in situ and satellite SST analysis for climate, *J. Clim.*, *15*, 1609–1625, doi:10.1175/1520-0442(2002)015<1609:AIISAS>2.0.CO;2.

Roach, W. T. (1995), Back to basics: Fog: Part 3—The formation and dissipation of sea fog, *Weather*, *50*, 80–84.

Roach, W. T., R. Brown, S. J. Caughey, J. A. Garland, and C. J. Readings (1976), The physics of radiation fog: I. A field study, *Q. J. R. Meteorol. Soc.*, *102*, 313–333.

Schmidli, J., C. Frei, and C. Schär (2001), Reconstruction of mesoscale precipitation fields from sparse observations in complex terrain, *J. Clim.*, *14*, 3289–3306, doi:10.1175/1520-0442(2001)014<3289:ROMPFF>2.0.CO;2.

Taylor, G. I. (1917), The formation of fog and mist, *Q. J. R. Meteorol. Soc.*, *43*, 241–268.

Torrence, C., and G. P. Compo (1998), A practical guide to wavelet analysis, *Bull. Am. Meteorol. Soc.*, *79*, 61–78, doi:10.1175/1520-0477(1998)079<0061:APGTWA>2.0.CO;2.

Weng, H., and K.-M. Lau (1994), Wavelets, period doubling, and time frequency localization with application to organization of convection over the tropical western Pacific, *J. Atmos. Sci.*, *51*, 2523–2541, doi:10.1175/1520-0469(1994)051<2523:WPDATL>2.0.CO;2.

Whiffen, B. (2001), Fog: Impact on aviation and goals for meteorological prediction, paper presented at Second Conference on Fog and Fog Collection, Environ. Canada, St. John's, Newfoundland, Canada.

Whiffen, B., P. Delannoy, and S. Siok (2003) Fog: Impact on road transportation and mitigation options, paper presented at 10th World Congress and Exhibition on Intelligent Transportation Systems and Services, ERTICO-ITS Europe, Madrid, Spain.

Wilks, D. (1995), *Statistical Methods in the Atmospheric Sciences: An Introduction*, 467 pp., Academic, San Diego, Calif.

Won, D. J., S. Y. Kim, K. E. Kim, and K. D. Min (2000), Analysis of meteorological and oceanographic characteristics on the sea fog over the Yellow Sea (in Korean), *J. Korean Meteorol. Soc.*, *36*, 631–642.

Zhang, S.-P., S.-P. Xie, Q.-Y. Liu, Y.-Q. Yang, X.-G. Wang, and Z.-P. Ren (2009), Seasonal variations of Yellow Sea fog: Observations and mechanisms, *J. Clim.*, doi:10.1175/2009JCLI2806.1.

D.-E. Chang, H.-S. Lee, J.-S. Lee, and Y. H. Lee, Forecast Research Laboratory, National Institute of Meteorological Research, Korea Meteorological Administration, 45 Gisangcheong-gil, Dongjak-gu, Seoul 156-720, Republic of South Korea.

S. K. Park, Department of Environmental Science and Engineering, Ewha Womans University, 11-1 Daehyun-dong, Seodaemun-gu, Seoul 120-750, Republic of Korea. (spark@ewha.ac.kr)